Monodispersed Microbubble Formation Using Microchannel Technique

Motohiro Yasuno, Shinji Sugiura, Satoshi Iwamoto, and Mitsutoshi Nakajima
National Food Research Institute, Tsukuba, Ibaraki, 305-8642 Japan

Atsushi Shono and Kazumi Satoh
Dept. of Industrial Chemistry, Tokyo University of Science, Shinjuku, Tokyo, 162-8601 Japan

DOI 10.1002/aic.10276
Published online in Wiley InterScience (www.interscience.wiley.com).

Recently, we proposed microchannel (MC) emulsification, a novel method for making monodispersed emulsion with a coefficient of variation (CV) less than 5%. In this study, we attempted monodispersed microbubble formation using the MC technique. Monodispersed microbubbles were formed using surfactants and proteins as dispersing agent. The average bubble size ranged from 33.6 to 51.1 μm, and CV values were below 10%. The bubble formation behavior was compared with the droplet formation behavior. The microbubble formation appears to be based on the spontaneous transformation caused by surface tension, as previously shown for liquid–liquid systems. The average bubble size was affected by viscosity, which is consistent with the results for the liquid–liquid system in previous studies. In the case of protein, the effect of surface viscoelasticity was indicated, which was not reported for the liquid–liquid system. © 2004 American Institute of Chemical Engineers *AIChE J,* 50: 3227–3233, 2004

Keywords: microchannel, monodispersed microbubbles, microbubble formation, microscope video system, monodispersed emulsion

Introduction

In the last decade of the twentieth century, microfabrication technologies have considerably advanced with the progress of electronic industries. Recently, the application of micromachining techniques has grown rapidly in various fields. New applications are appearing in biotechnology and chemical reactions, such as polymerase chain reaction on a chip (Kopp et al., 1997), DNA analysis (Burns et al., 2000; Chou et al., 1999), cell handling (Li and Harrison, 1997; Takayama et al., 1999), and microchemical reactors (Jensen, 1999; Srinivasan et al. 1997). These microelectromechanical systems have the advantages of precise fabrication, replication by photolithography, small volume, portability, small amounts of expensive reagents, short reaction and analysis times, and little waste. Fluid dynamics on a micrometer scale feature significant effects such as viscosity and interfacial tension, laminar flow, and fast diffusion (Jensen, 1999; Sammarco and Burns, 1999). Applying these features, microfabricated devices for pumping discrete droplets (Sammarco and Burns, 1999), blood rheology (Kikuchi et al., 1992), micromixing (Ehrfeld et al., 2000), and diffusion-based separation and detection (Weigl and Yager, 1999) have been developed.

We proposed a novel method for making monodispersed emulsion droplets from a microfabricated channel array (Kawakatsu et al., 1997). This emulsification technique is called microchannel (MC) emulsification. Emulsion with a coefficient of variation below 5% (Kawakatsu et al., 1997) and droplet sizes ranging from 3 to 100 μm have been successfully prepared by applying this technique (Kobyashi et al., 2001; Sugiura et al., 2002a). The droplet size was affected by the geometry of MC (Sugiura et al., 2002b) and viscosity of both

M. Yasuno is also affiliated with Research and Development Center, Showa Sangyo Co., Ltd., Funabashi, Chiba, 273-0015 Japan.
Correspondence concerning this article should be addressed to M. Nakajima at mnaka@affrc.go.jp.

phases (Kawakatsu et al., 2000). This technique is promising not only for preparing emulsions but also for a variety of systems. We have applied it to preparing several types of oil-in-water emulsions, water-in-oil emulsions (Sugiura et al., 2001a), lipid microparticles (Sugiura et al., 2000), polymer microparticles (Sugiura et al., 2001b, 2002c), and microcapsules. Thus, there were many investigations with respect to liquid–liquid systems using MC technique, although until now there has been an absence of research regarding gas–liquid system using the MC technique. Therefore, there was uncertainty whether monodispersed microbubbles, which constitute a gas–liquid dispersion, were formed using the MC technique.

Monodispersed microbubbles are useful for fundamental studies because the interpretation of experimental results is much simpler than that for polydispersed microbubbles. They can also serve as useful systems for measuring important properties of microbubbles. For example, the stability of microbubbles can be monitored very simply because changes in the bubble size are easily studied by having monodispersed microbubbles. Monodispersed microbubbles can greatly reduce Ostwald ripening by reducing the effective Laplace pressure difference because the microbubbles are identical in size. In addition, monodispersed microbubble formation was an expected application of a column of microbubbles and contrast agent. A flotation column of microbubbles was investigated for cleaning micronized coals (Choung and Luttrell et al., 1993; Li et al., 2003). Microbubbles are in clinical use as echo-contrast agents for sonographic application (Grinstaff and Suslick, 1991; Skyba and Kaul 2000). Microbubbles having a liquid–gas interface are able to backscatter incident ultrasound.

In the present study, we attempted monodispersed microbubble formation using the MC technique. We investigated the parameters affecting microbubble formation, such as dispersing agent, surface tension, and viscosity. Microbubble formation behavior was also compared with the droplet formation behavior in a liquid–liquid system using the MC technique.

Experimental

Materials

Air was used as the dispersed phase for microbubble formation. Phosphate buffer (25 mmol/L) was used as the continuous phase. We used surfactants and proteins as dispersing agent. Sodium dodecyl sulfate (SDS) and polyoxyethylene (20) sorbitan monolaurate (Tween 20) were purchased from Wako Pure Chemicals (Osaka, Japan) and used as surfactant. Sodium caseinate and bovine serum albumin (BSA, catalog no. A4503) were purchased from Wako Pure Chemicals and Sigma Chemical Co. (St. Louis, MO), respectively, and used as protein. SDS concentrations ranged from 0.01 to 0.3 wt % to control surface tension. Tween 20 and protein concentrations of 1.0 wt %, which exceed the critical micelle concentration (CMC), were used. Poly(ethylene glycol) (PEG) was obtained from Wako Pure Chemicals and used to control the viscosities of the continuous phase. For comparison, a liquid–liquid emulsion system was also tested, in which decane was used as the dispersed phase and 0.3 wt % SDS aqueous solution was used as the continuous phase.

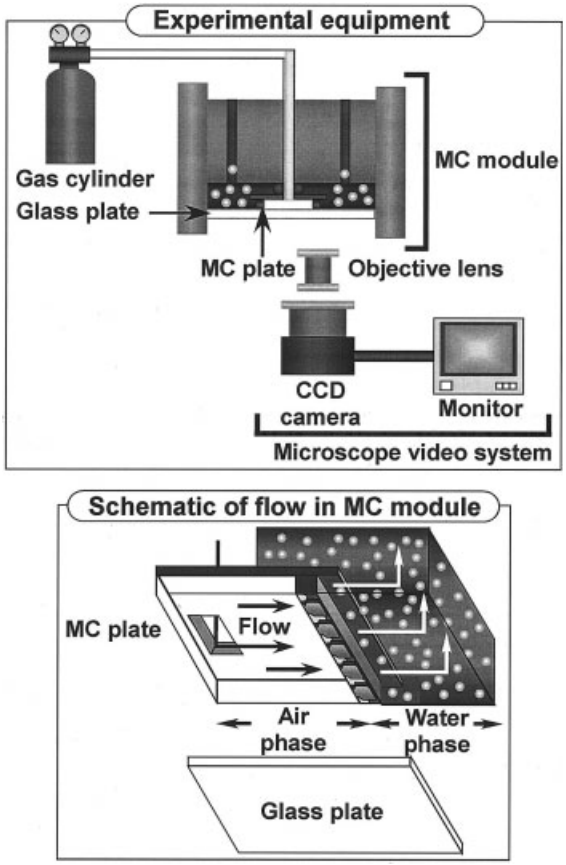

Figure 1. Experimental equipment and schematic of flow of the dispersed air phase through the silicon.

Microbubbles and droplet formation using MC technique

Figure 1 shows the experimental equipment used in this study and schematic flows of the dispersed air phase and continuous water phase in the MC module. The experimental equipment consists of a microscope video system, a silicon MC, an MC module, and the gas cylinder. The microbubble formation process was observed in real time through a glass plate in an MC module. The observed image was detected by using a charge-coupled device (CCD) camera (HV-C20M, Hitachi, Tokyo, Japan) and recoded by digital video player (WV-DR5, Sony Corp., Tokyo, Japan) with a total magnification of 1000. Figure 2 shows the schematic of the MC plate used in this study. The silicon MC plate was fabricated using photolithography and orientation-dependent etching. The silicon MC plate was 15 $\times$ 15 mm, and a 1-mm-diameter hole was produced at the center of the plate. Four terrace lines, with a height of 100 μm and a length of 10 mm, were fabricated on the MC plate. MCs were fabricated on each terrace line. The total number of MCs was 600. MC width and depth were 16 and 4 μm, respectively.

The MC module was initially filled with the continuous phase. The dispersed air phase was pressurized by the gas cylinder. The pressurized dispersed air phase entered the space between the silicon MC plate and the glass plate, and microbubbles were formed from the MC.

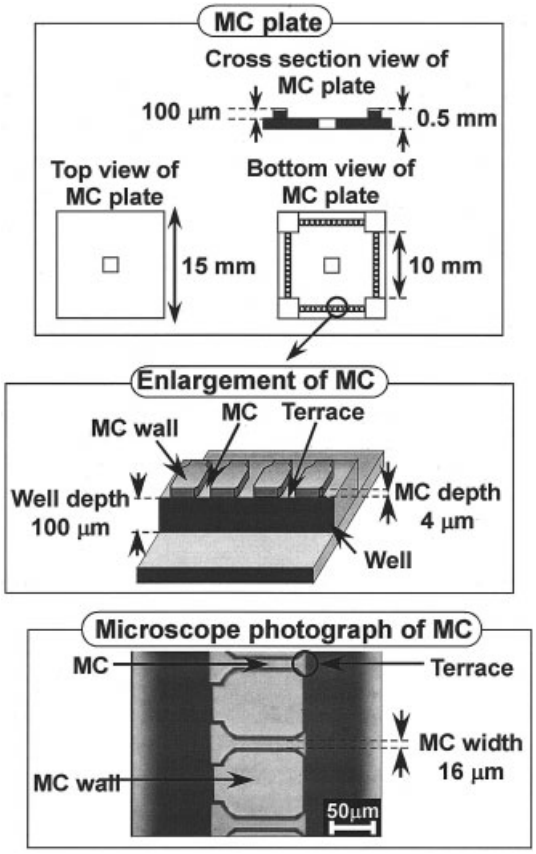

Figure 2. Silicon MC plate used in this study.

In the case of the liquid–liquid system using the MC technique, the dispersed oil phase was pressurized by changing the height of the liquid chamber. The pressurized dispersed oil phase entered the space between the silicon MC plate and the glass plate. The other experimental equipment was the same as that used for microbubble formation.

Measurement and analytical method

The average bubble and droplet size and the coefficient of variation (CV) were determined by measuring the sizes of 100 microbubbles and droplets from recorded pictures using Winroof software (Mitani Corp., Fukui, Japan). CV can be defined by the following equation

$$\mathrm{CV} = \frac{\delta}{d_{av}} \times 100 \qquad (1)$$

where CV is the coefficient of variation (%), δ is the standard deviation, and d_{av} is the average bubble and droplet size.

The surface tension and interfacial tension were measured by the pendant droplet method using a fully automatic interfacial tensiometer (PD-W; Kyowa Interface Science Co., Saitama, Japan). The viscosity of the continuous phase was measured with Cannon–Fenske viscometers. The density was measured with picnometers. The pH of the continuous phase was measured with Digital-pH-Meter (E632, Shibata Co., Tokyo, Japan). These measurements were investigated at room temperature.

Results and Discussion

Monodispersed microbubble formation using the MC technique

Monodispersed microbubble formation was tested by pressurizing the air into the continuous phase through MC. We investigated the effect of continuous phase on microbubble formation using the MC technique. Water, 0.3 wt % SDS, 1.0 wt % Tween 20, 1.0 wt % sodium caseinate, and 1.0 wt % BSA aqueous solution were tested as continuous phases. Table 1 shows the properties of continuous phases used in this study. The viscosity and pH of these continuous phases were almost identical. The surface tension of these continuous phases varied from 36.2 to 69.3 mN/m. Water had the highest surface tension value, and 0.3 wt % SDS aqueous solution had the lowest value in these continuous phases. The microbubble formation behaviors were classified into two cases, as shown in Figure 3. Figure 3A shows microphotographs of microbubble formation using the MC technique when the continuous phase was water. In this case, it was difficult to form monodispersed microbubbles because formed microbubbles immediately coalesced at the outside end of the MC. Figure 3B shows microbubble formation using the MC technique when the continuous phase was 0.3 wt % SDS aqueous solution. Monodispersed microbubbles were successfully formed. In the case of 1.0 wt % Tween 20, sodium caseinate, and BSA aqueous solution, monodispersed microbubbles were also formed when air broke through the MC. Figure 4 shows images of monodispersed microbubbles formed using surfactants and protein aqueous solution as the continuous phase. The formed microbubbles had spherical shape with regular size. In conventional bubble formation method using nozzle, orifice, stirring, and so on, bubble size formed by these methods was more irregular than that formed by the MC technique.

Figure 5 shows bubble size distributions of microbubbles formed by using surfactants and protein aqueous solutions as the continuous phase. The average bubble size and CV of microbubbles were 33.6 μm and 1.8% for 0.3 wt % SDS aqueous solution; 39.1 μm and 3.4% for 1.0 wt % Tween 20 aqueous solution; 48.9 μm and 5.0% for 1.0 wt % sodium caseinate aqueous solution; and 51.1 μm and 7.5% for 1.0 wt % BSA aqueous solution. CV values for surfactant aqueous solutions were lower than those for protein aqueous solutions, whereas CV values for protein aqueous solutions were below 10%. In addition, the average bubble sizes for protein aqueous solutions were larger than those for surfactant aqueous solutions. The viscosity and pH of surfactant and protein aqueous

Table 1. Properties of Continuous Phases Used in This Study

Continuous Phase	Surface Tension (mN/m)	Viscosity (mPa · s)	pH
Water*	69.3	0.9	7.1
0.3 wt % SDS*	36.2	0.9	7.1
1.0 wt % Tween 20*	39.7	0.9	7.1
1.0 wt % Sodium caseinate*	49.2	1.1	7.0
1.0 wt % BSA*	59.1	0.9	7.0

*25 mmol/L phosphate buffer.

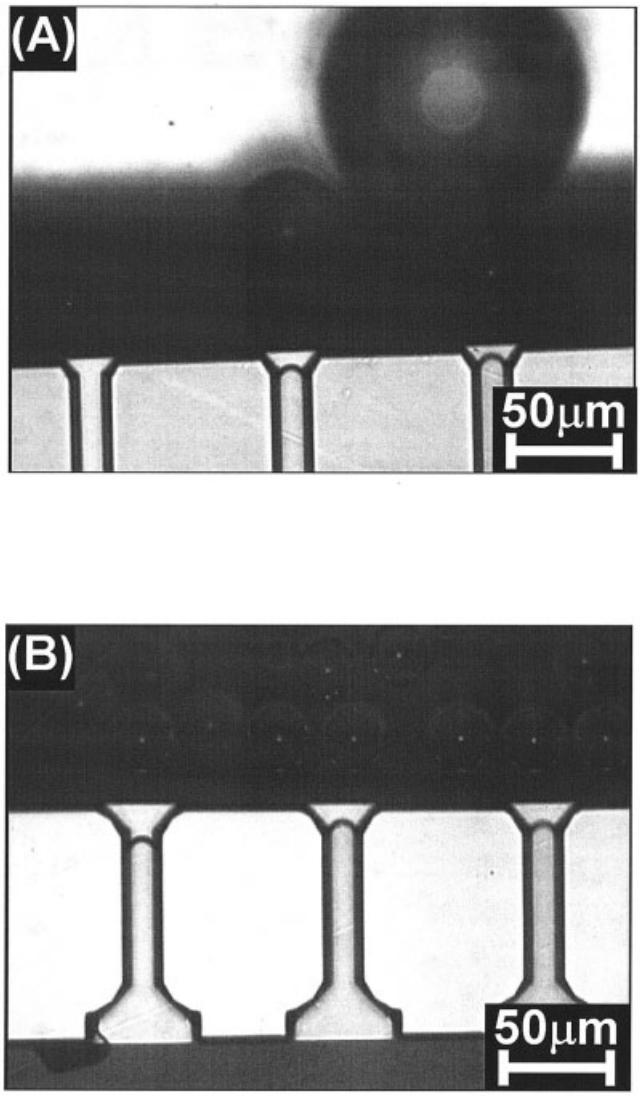

Figure 3. Microphotographs of microbubble formation using MC.

(A) The continuous phase was water. Microbubbles were created, but they coalesced immediately. (B) The continuous phase was 0.3 wt % SDS aqueous solution. Monodispersed microbubbles successfully formed.

solutions were almost identical, whereas there was a considerable difference in the surface tension among these solutions. The previous studies for liquid–liquid systems show that the droplet size is affected by viscosity (Kawakatsu et al., 2001) and is not affected by interfacial tension (Tong et al., 2000). Therefore, we investigated the effect of surface tension and viscosity in detail, the discussion of which is presented below.

Comparison of gas–liquid system and liquid–liquid system using the MC technique

We investigated both gas–liquid and liquid–liquid systems using the MC technique when the continuous phase was 0.3 wt % SDS aqueous solution. Figure 6A shows the droplet formation behavior of liquid–liquid system using the MC technique. Monodispersed droplets were formed when the dispersed phase broke through the MC. The droplet formation behavior was almost identical to microbubble formation behavior. To understand microbubbles and droplet formation behaviors observed in this study, we will discuss the droplet-formation model using MC, proposed in our previous study (Sugiura et al., 2001c). In the model, the droplets were formed by spontaneous transformation caused by interfacial tension. Therefore, the droplets were formed without the continuous-phase flow. We considered the droplet formation also applied to the microbubble formation because the microbubbles formed without continuous-phase flow. However, the average rate of droplet formation was slower than that of microbubbles. This is because there was a substantial difference in dispersed-phase viscosity and in surface and interfacial tension.

Figure 6B shows an image of monodispersed droplets formed under the condition of Figure 6A. The formed droplets were of almost the same characteristics as microbubbles formed under condition of Figure 4A. The average bubble size was 33.6 μm, more than twice the average droplet size of 14.4 μm. Table 2 shows a comparison of the dispersed-phase viscosity, surface and interfacial tension, the average bubble and droplet sizes, and CV. The surface tension for the gas–liquid system was higher than that for the liquid–liquid system, whereas the dispersed-phase viscosity for the gas–liquid system was lower than the interfacial tension for the liquid–liquid system. We discuss the difference in the average bubble size and the average droplet size in the following section.

Effect of surface/interfacial tension and continuous-phase viscosity on the average bubble and droplet size

We investigated the effect of surface tension on the average bubble size formed by using different concentrations of SDS aqueous solutions. Figure 7 shows the effect of surface tension on the average bubble size when the continuous phases constituted different SDS concentrations, 1.0 wt % Tween 20, 1.0 wt % sodium caseinate, and 1.0 wt % BSA aqueous solutions. The average bubble sizes were almost identical in the SDS concentration range of 0.02–0.3 wt % (surface tension range of 36.2–48.9 mN/m). However, it was found that the average bubble sizes formed by using 1.0 wt % sodium caseinate and 0.02 wt % SDS (surface tension of 48.9 mN/m) aqueous solutions were considerably different, even though they have almost the same surface tension.

Next, we investigated the effect of continuous-phase viscosity on the average bubble size. Figure 8 shows the effect of viscosity ratio of the dispersed phase to the continuous phase on the average bubble size when the continuous phases were different concentrations of PEG aqueous solutions containing 0.3 wt % SDS. The continuous-phase viscosities ranged from 0.9 to 10.9 mPa·s. The average bubble size decreased with increasing viscosity ratio. In other words, the average bubble size increased with increasing continuous-phase viscosity.

In addition, we plotted the average droplet size formed under conditions of Table 2 in Figure 8. The average bubble/droplet size was inversely proportional to the viscosity ratio. The linear relation between the average size and viscosity ratio was obtained by the following equation

$$\log D = -0.27 \log \eta + 1.13 \qquad (2)$$

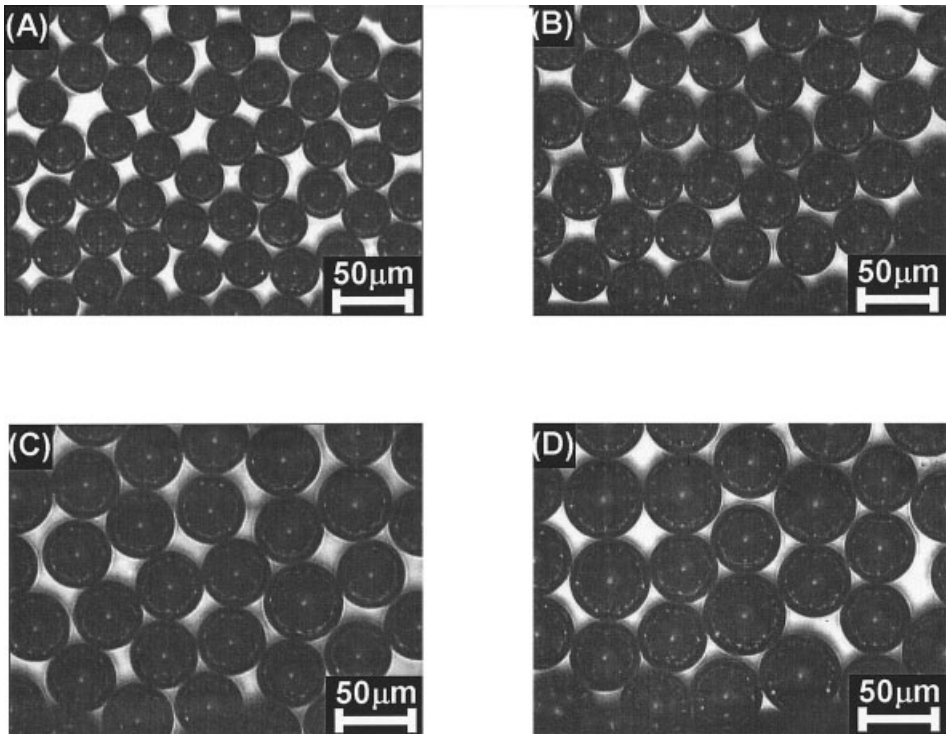

Figure 4. Images of monodispersed microbubbles formed using MC under different continuous phases.

The continuous phases were 0.3 wt % SDS aqueous solution (A), 1.0 wt %Tween 20 aqueous solution (B), 1.0 wt % sodium caseinate aqueous solution (C), and 1.0 wt % BSA aqueous solution (D).

where D is the average size and η is the viscosity ratio of the dispersed phase to the continuous phase. The correlation coefficient was 0.988. This good correlation means that the difference between the average bubble size and the average droplet size is well explained by the viscosity difference. Previous studies for liquid–liquid systems reported that the droplet size was affected by the viscosities of both phases (Kawakatsu et al., 2001) and independent of the interfacial tension (Tong et al., 2000). With respect to the microbubble formation using SDS, the average bubble size was not affected by the surface tension in the SDS concentration range of 0.02–0.3 wt % (surface tension range of 36.2–48.9 mN/m), and the average bubble size increased with increasing continuous-phase viscosity. These experimental results showed good agreement with the results shown in the previous study. However, in the case of protein, the bubble size was larger than that for the SDS system, even though the viscosity of protein aqueous solution has almost the same value as that of the SDS aqueous solution. In addition, in the case of 0.01 wt % SDS (surface tension of 54.9 mN/m) aqueous solution, the average bubble size was slightly higher than that of higher-concentration SDS aqueous solution. These results are inconsistent with the previous study, which would be interpreted by dynamic interfacial behavior, such as interfacial viscoelasticity and dynamic interfacial tension.

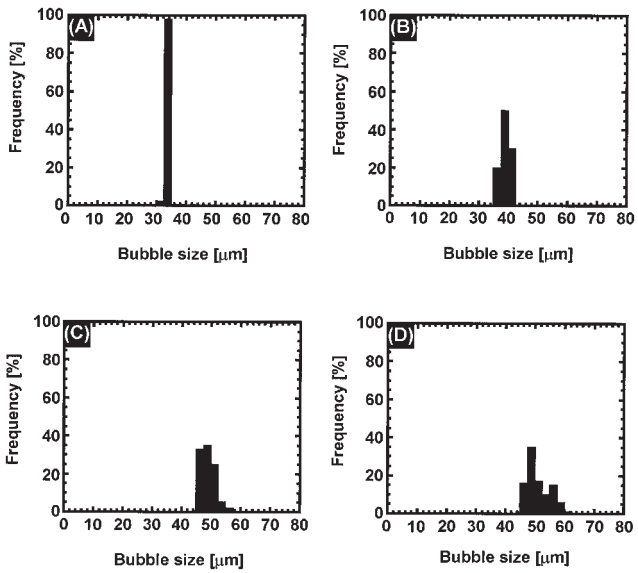

Figure 5. Bubble size distribution.

The continuous phases were 0.3 wt % SDS aqueous solution (A), 1.0 wt % Tween 20 aqueous solution (B), 1.0 wt % sodium caseinate aqueous solution (C), and 1.0 wt % BSA aqueous solution (D).

If the transport of surfactant between bulk solution and interface by convective flow and diffusion is slower than both the surface extension of bubbles and their breakup, the dynamic interfacial behavior is not negligible. The dynamic interfacial properties, including interfacial viscoelasticity and dynamic interfacial tension, depend on the rate of the surfactant transport to the newly created interface. In the present system, this transport is determined by diffusional transfer because microbubble formation using the MC technique was carried out without the continuous-phase flow. The effect of diffusional

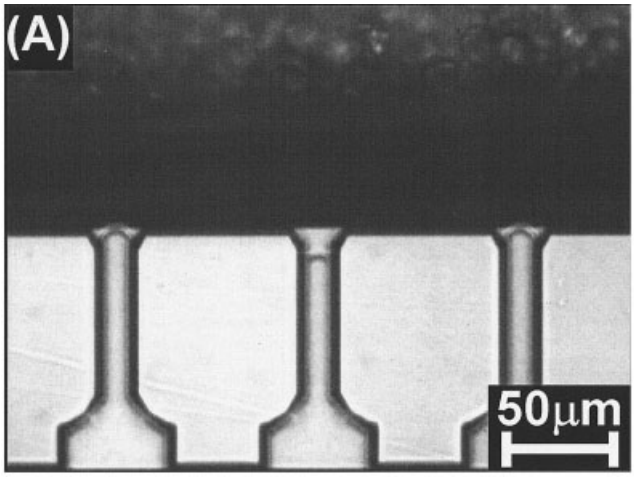

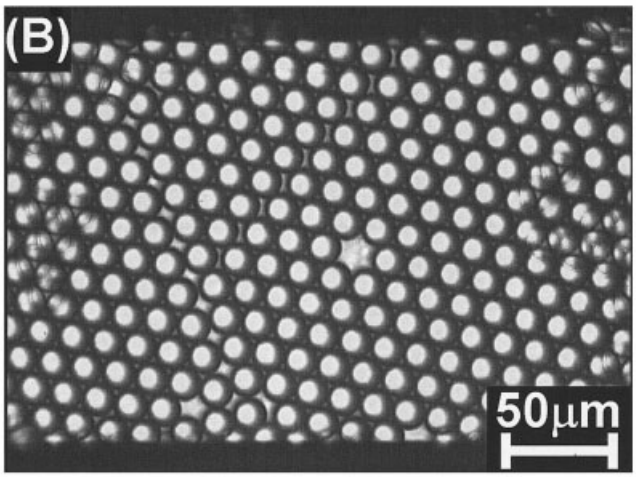

Figure 6. Microphotographs of droplet formation using MC (A) and monodispersed droplets formed using MC (B).

The dispersed oil phase was decane. The continuous phase was 0.3 wt % SDS aqueous solution.

transfer is evaluated by the timescale of diffusion τ_d, compared with the time for bubble formation. The adsorption kinetics for the ionic surfactant has been studied (Sasaki et al., 1977; Vlahovska et al., 1997), although it is not as simple as the nonionic surfactant because of the existence of an electrical double layer. The theoretical model predicts τ_d to be on the order of 10^{-3}–10^{-4} s for an SDS concentration of 0.03%

Table 2. Comparison of the Dispersed-Phase Viscosity, Surface and Interfacial Tension, Average Bubble and Droplet Size, and CV

Dispersed Phase	Dispersed-Phase Viscosity (mPa · s)	Surface/Interfacial Tension (mN/m)	Average Bubble/ Droplet Size (μm)	CV (%)
Air	0.02	36.2*	33.6*	1.8
Decane	0.84	6.0*	14.4*	2.8

*Continuous phase is 0.3 wt % SDS.

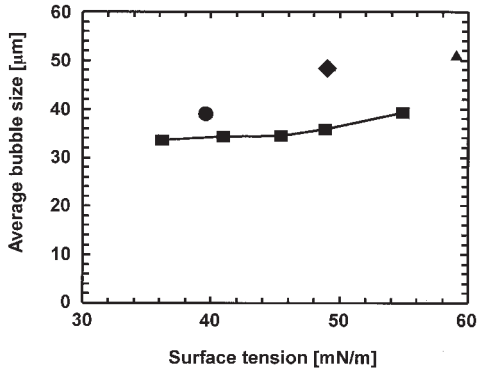

Figure 7. Effect of surface tension on the average bubble size.

The continuous phases constituted different concentrations of SDS aqueous solutions (■), 1.0 wt % Tween 20 aqueous solution (●), 1.0 wt % sodium caseinate aqueous solution (◆), and 1.0 wt % BSA aqueous solution (▲). SDS concentrations of 0.01, 0.02, 0.03, 0.05, and 0.3 wt % were used.

(Vlahovska et al., 1997). Measurements by the capillary-wave method (Sasaki et al., 1977) also yield an adsorption relaxation time on the order of 10^{-3} s for SDS in the concentration ranges similar to those used in our experiment (Sasaki et al., 1977). On the other hand, it was reported that τ_d for BSA of 4.8 g/L concentration was 1.3 s (Serrien et al., 1992).

The time for bubble formation was less than 1/600 s, which is the detection limit of the high-speed camera in our laboratory. In the case of protein, dynamic interfacial behavior may affect the bubble size because τ_d for protein seems significantly longer compared with the bubble formation time. During conventional emulsification, the interfacial tension gradients enable the interface to resist tangential stresses from the adjoining flowing liquid, and interfacial viscoelasticity is capable of increasing the effective viscosity by more than an order of magnitude, under specified conditions (Lucassen-Reynders and Kuijpers, 1992). In the case of protein, we consider that the interfacial viscoelasticity resists movement of interface, and a great amount of air flows into the well during microbubble formation. Consequently, the larger microbubbles were formed

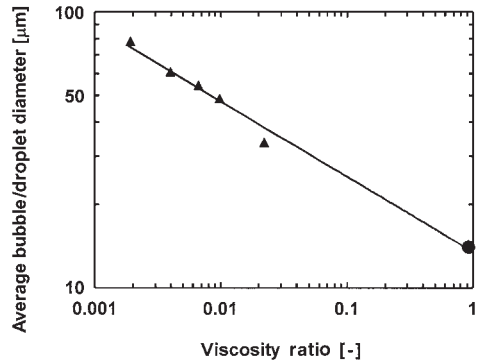

Figure 8. Effect of the viscosity ratio of dispersed-phase viscosity to continuous-phase viscosity on the average bubble size (▲) and the average droplet size (●).

The continuous phase was 0.3 wt % SDS aqueous solution and different PEG concentrations.

using protein. Although the dynamic interfacial tension might be considerable for the microbubble formation for protein, we consider that dynamic interfacial tension does not affect the bubble size because droplet size was independent of the interfacial tension (Tong et al., 2000).

On the other hand, in the case of SDS, the dynamic interfacial behavior is negligible because τ_d for SDS would be shorter compared with the microbubble formation time. In the case of 0.01 wt % (surface tension of 54.9 mN/m) SDS aqueous solution, a slightly larger microbubble was formed than that for 0.02–0.3 wt % SDS aqueous solution. In this case, the dynamic interfacial behavior might affect the bubble size.

Conclusions

Formation of monodispersed microbubbles, using MC technique when the continuous phase was surfactant or protein aqueous solution, was successfully carried out. The average bubble size range was from 33.6 to 51.1 μm. The formed microbubbles were monodispersed in which CV was below 10% in the case of surfactant or protein aqueous solution. The bubble formation behavior was almost identical to the droplet formation behavior. The bubble formation appears to be based on the spontaneous transformation caused by surface tension, as reported previously for liquid–liquid system. The average bubble size increased with increasing continuous-phase viscosity. The average bubble size was almost independent of the surface tension in the case of SDS concentration from 0.02 to 0.3 wt %. The results were consistent with the results for the liquid–liquid system. However, the bubble size using protein was larger than that for SDS, even though the viscosity of the protein solution is almost the same value as that for SDS. The difference was explained by the effect of interfacial viscoelasticity.

Acknowledgment

This work was supported by the Nanotechnology Project of the Ministry of Agriculture, Forestry and Fisheries, Japan, as well as a Grant-in-Aid for Science Research from the Ministry of Education, Culture, Sports, Science, and Technology.

Literature Cited

Burns, M. A., B. N. Johnson, S. N. Brahmasandra, K. Hanhdique, J. R. Webster, M. Krishnan, T. S. Sammarco, P. M. Man, D. Jones, D. Heldsinger, C. H. Mastrangelo, and D. T. Burke, "An Integrated Nanoliter DNA Analysis Device," *Science*, **282**, 484 (2000).

Chou, H. P., C. Spence, A. Schere, and S. Quake, "A Microfabricated Device for Sizing and Sorting DNA Molecules," *Proc. Natl. Acad. Sci. U.S.A.*, **96**, 11 (1999).

Choung, J. W., G. H. Luttrell, and R. H. Yoon, "Characterization of Operating Parameters in the Cleaning Zone of Microbubble Column Flotation," *Int. J. Miner. Process*., **39**, 31 (1993).

Ehrfeld, W., V. Hessel, and H. Löwe, *Microreactors*, Wiley–VCH, Weinheim, Germany (2000).

Grinstaff, M. W., and K. S. Suslick, "Air-Filled Proteinaceous Microbubles: Synthesis of an Echo-Contrast Agent," *Proc. Natl. Acad. Sci. U.S.A.*, **88**, 7708 (1991).

Jensen, K. F. "Microchemical Systems: Status, Challenges, and Opportunities," *AIChE J.*, **45**, 2051 (1999).

Kawakatsu, T., H. Komori, M. Nakajima, Y. Kikuchi, and T. Yonemoto, "Regular-Sized Cell Creation in Microchannel Emulsification by Visual Microprocessing Method," *J. Am. Oil Chem. Soc.*, **74**, 317 (1997).

Kawakatsu, T., G. Trägårdh, Ch. Trägårdh, M. Nakajima, N. Oda, and T. Yonemoto, "The Effect of the Hydrophobicity of Microchannels and Components in Water and Oil Phases on Droplet Formation in Microchannel Water-in-Oil Emulsification," *Colloids Surf. A*, **179**, 29 (2001).

Kikuchi, Y., Sato, K., Ohki, H., Kaneko, T. "Optically Accessible Microchannels Formed in a Single-Crystal Silicon Substrate for Studies of Blood Rheology," *Microvasc. Res.*, **44**, 226 (1992).

Kobyashi, I., M. Nakajima, H. Nabetani, Y. Kikuchi, A. Shono, and K. Satoh, "Preparation of Micron-Scale Monodisperse Oil-in-Water Microspheres by Microchannel Emulsification," *J. Am. Oil Chem. Soc.*, **78**, 797 (2001).

Kopp, M. U., A. J. de Mello, and A. Manz, "Chemical Amplification: Continuous-Flow PCR on a Chip," *Science*, **280**, 1046 (1997).

Li, B., D. Tao, Z. Ou, and J. Liu, "Cyclo-Microbubble Column Flotation of Fine Coal," *Sep. Sci. Technol*., **38**, 1125 (2003).

Li, P. C., and D. J. Harrison, "Transport, Manipulation, and Reaction of Biological Cells on-Chip Using Electrokinetic Effects," *Anal. Chem.*, **69**, 1564 (1997).

Lucassen-Reynders, E. H., and K. A. Kuijpers, "The Role of Interfacial Properties in Emulsification," *Colloids Surf*., **65**, 175 (1992).

Sammarco, T. S., and M. A. Burns, "Thermocapillary Pumping of Discrete Drops in Microfabricated Analysis Devices," *AIChE J.* **45**, 350 (1999).

Sasaki, M., T. Yasunaga, and N. Tatsumoto, "Relaxation Studies of the Adsorption–Desorption Equilibrium of Surfactants on the Gas–Liquid Interface. II. Experimental Studies," *Bull. Chem. Soc. Jpn.*, **50**, 858 (1977).

Serrien, G., G. Geeraerts, L. Ghosh, and P. Joos, "Dynamic Surface Properties of Adsorbed Protein Solutions: BSA, Casein and Buttermilk," *Colloids Surf.*, **68**, 219 (1992).

Skyba, D. M., and S. Kaul, "Advances in Microbubble Technology," *Coron. Artery Dis*., **11**, 211 (2000).

Srinivasan, R., I. M. Hsing, P. E. Berger, and K. F. Jensen, "Micromachined Reactors for Catalytic Partial Oxidation Reactions," *AIChE J.*, **43**, 3059 (1997).

Sugiura, S., M. Nakajima, H. Itou, and M. Seki, "Synthesis of Polymeric Microspheres with Narrow Size Distribution Employing Microchannel Emulsification," *Macromol. Rapid Commun.*, **22**, 773 (2001b).

Sugiura, S., M. Nakajima, S. Iwamoto, and M. Seki, "Interfacial Tension Driven Monodispersed Droplet Formation from Microfabricated Channel Array," *Langmuir*, **17**, 5562 (2001).

Sugiura, S., M. Nakajima, and M. Seki, "Preparation of Monodispersed Emulsion with Large Droplets Using Microchannel Emulsification," *J. Am. Oil Chem. Soc.*, **79**, 515 (2002a).

Sugiura, S., M. Nakajima, and Seki, M. "Prediction of Droplet Diameter for Microchannel Emulsification," *Langmuir*, **18**, 3854 (2002b).

Sugiura, S., M. Nakajima, and Seki, M. "Preparation of Monodispersed Polymeric Microspheres over 50 μm Employing Microchannel Emulsification," *Ind. Eng. Chem. Res.*, **41**, 4043 (2002c).

Sugiura, S., M. Nakajima, J. Tong, H. Nabetani, and M. Seki, "Preparation of Monodispersed Solid Lipid Microspheres Using a Microchannel Emulsification Technique," *J. Colloid Interface Sci.*, **227**, 95 (2000).

Sugiura, S., M. Nakajima, H. Ushijima, K. Yamamoto, and M. Seki, "Preparation Characteristics of Monodispersed Water-in-Oil Emulsions Using Microchannel Emulsification," *J. Chem. Eng. Jpn.*, **34**, 757 (2001a).

Takayama, S., J. C. McDonald, E. Ostuni, M. N. Liang, P. J. A. Kenis, R. F. Ismagilov, and G. M. Whitesides, "Patterning Cells and Their Environments Using Multiple Laminar Fluid Flows in Capillary Networks," *Proc. Natl. Acad. Sci. U.S.A.*, **96**, 5545 (1999).

Tong, J., M. Nakajima, H. Nabetani, and Y. Kikuchi, "Surfactant Effect on Production of Monodispersed Microspheres by Microchannel Emulsification Method," *J. Surfact. Deterg.*, **3**, 285 (2000).

Vlahovska, P. M., K. D. Danov, A. Mehreteab, and G. Broze, "Adsorption Kinetics of Ionic Surfactants with Detailed Account for the Electrostatic Interactions," *J. Colloid Interface Sci.*, **192**, 194 (1997).

Weigl, B. H., and P. Yager, "Microfluidics: Microfluidic Diffusion-Based Separation and Detection," *Science*, **283**, 346 (1999).

Manuscript received Jul. 27, 2003, and revision received Apr. 6, 2004.